International Journal of Pharmaceutics, 85 (1992) 87–96

IJP 02778

Glass formation of 4″-*O*-(4-methoxyphenyl)acetyltylosin and physicochemical stability of the amorphous solid

Toshio Yamaguchi [a], Masami Nishimura [a], Rokuro Okamoto [a], Tomio Takeuchi [b] and Keiji Yamamoto [c]

[a] *Central Research Laboratories, Mercian Corporation, 9-1 Johnan 4 chome, Fujisawa 251 (Japan),* [b] *Institute of Microbioal Chemistry, 14-23 Kamiosaki 3 chome, Shinagawa-ku, Tokyo 141 (Japan) and* [c] *Faculty of Pharmaceutical Sciences, Chiba University, 1-33 Yayoicho, Inage-ku, Chiba 263 (Japan)*

(Received 25 October 1991)
(Modified version received 25 December 1991)
(Accepted 22 January 1992)

Key words: 4″-*O*-(4-Methoxyphenyl)acetyltylosin; Amorphous solid; Spray drying; Glassy state; Glass transition temperature; Recrystallization temperature; Stability

Summary

Glass formation of 4″-*O*-(4-methoxyphenyl)acetyltylosin (MAT) and the physicochemical stability of amorphous MAT have been investigated. The amorphous form of MAT was prepared by spray drying of an MAT dichloromethane solution. The glassy state was confirmed by DSC and the glass transition temperature was observed to be 102–103°C. It was found that different kinds of the glassy state of MAT could be obtained by changing the inlet temperature of spray drying. Storage experiments on amorphous powders at 40°C and 75% RH revealed that the amorphous powders prepared at a temperature between the glass transition (T_g) and recrystallization (T_c) temperatures were the most stable. A correlation between the stability and the apparent density was observed.

Introduction

4″-*O*-(4-Methoxyphenyl)acetyltylosin (MAT) is a new, 16-membered macrolide antibiotic derivative, in which the 4″-OH group of tylosin has been (4-methoxyphenyl)acetylated, as shown in Fig. 1 (Tsuchiya et al., 1982). MAT has a broad spectrum of antibacterial and also shows reasonable antibacterial activity against macrolide-resistants. MAT is very soluble in chloroform and dichloromethane, and sparingly soluble in methanol, however, the solubility of MAT in water is about 1.0 μg/ml at 37°C.

Low bioavailability is a common problem with poorly water-soluble drugs when orally administered (Ballard and Nelson, 1962; Yamamoto et al., 1976; Nakai, 1986). The dissolution behavior of the drug is influenced by the physicochemical state of the drug, including hydrate or solvate formation, polymorphism and variations in crystallinity (Haleblian and McCrone, 1969; Baba et al., 1990; Kawashima et al., 1991). There are a number of reports regarding the relationship be-

Correspondence to: T. Yamaguchi, Central Research Laboratories, Mercian Corporation, 9-1 Johnan 4 chome, Fujisawa 251, Japan.

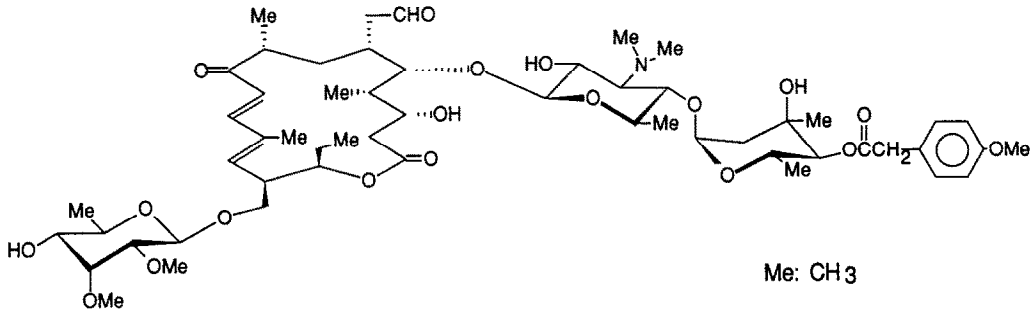

Fig. 1. Structure of 4″-*O*-(4-methoxyphenyl)acetyltylosin (MAT).

tween the dissolution behavior of different solid states and the bioavailability (Lindenbaum et al., 1973; Aoyagi et al., 1985; Morishita et al., 1988). In particular, distinct differences in bioavailability have been reported between the crystalline and amorphous forms of drugs for novobiocine and a number of other drugs (Mullins and Macek, 1960; Sato et al., 1981). The preparation of a stable amorphous solid form is important for designing dosage systems of poorly water-soluble drugs. The phenomenon of a glass transition shown by organic drugs has been reported by Fukuoka et al. (1989) and a number of glass-forming drugs have recently been discovered. However, there are few reports regarding the glass state of macrolide compounds.

In this work, the preparation of amorphous MAT by the spray drying method was investigated. We also examined the physicochemical stability of amorphous MAT during storage, and discuss the factors influencing the stability of the amorphous state.

Experimental

Materials

MAT (crystalline) was prepared in the Central Research Laboratories of Mercian Corp. Dichloromethane of extra-pure grade was purchased from Junsei Chemical Co., Ltd.

Preparation of amorphous solid

The amorphous solid form of MAT was obtained by spray drying dichloromethane solutions of MAT using an SD-1 spray dryer (Tokyo Rikakikai Co., Ltd; spray, nozzle type; drying temperature, 50–160°C). The concentration of MAT was 100 mg/ml, and the supply speed of dichloromethane solutions of MAT was 12.0 ml/min. The air pressure was 1.0 kg/cm^2.

Powder X-ray diffractometry

Powder X-ray diffraction patterns were determined with an X-ray diffractometer (JDX-8030, Nihon Denshi Co. Ltd, CuKα, 40 kV/20 mA, $2\theta = 5.0$–$40.0°$).

Infrared spectroscopy

A Hitachi model 260-30 IR spectrophotometer was used. Measurements were carried out using KBr disks.

Thermal analysis (DSC)

DSC measurements were performed under semi-closed conditions using a Shimadzu model DSC-50 differential scanning calorimeter. Aluminum lids were used except when observing changes in appearance of samples in the DSC measurements. The heating rate was 10°C/min and nitrogen gas flow amounted to 50 ml/min.

Measurement of apparent density

A 30 cm^3 container was weighed on a 160 g capacity balance. A powder funnel with a sieve (10 mesh) was placed in the container and a powder was poured carefully into it until the level reached 30 cm^3. The weight of the container plus powder minus the tare was denoted 30-times the apparent density.

Dissolution studies

Dissolution patterns were obtained using a Nihon Bunko DT-610 type automatic dissolution apparatus. Distilled water, JP 1st fluid (pH 1.2) and JP 2nd fluid (pH 6.8) were used as the dissolution media. 500 ml of the dissolution medium was placed in a water-jacketed cell maintained at 37 ± 0.1°C, then 50 mg of the sample powder was added. At intervals of 2 min, 20-ml samples of the solution were passed through a G-3 filter and sent out to the unit cell. The concentration of MAT was determined based on the absorbance at $\lambda = 289$ nm. The sampling solution was returned to the original solution by the circulation system.

HPLC analysis

The potency and relative purity of MAT were determined by high-performance liquid chromatography (HPLC). The conditions for HPLC were as follows: apparatus, Shimadzu model LC-9A HPLC analyzer; detector, UV spectrophotometer ($\lambda = 280$ nm); column, 150 mm × 6 mm diameter stainless column packed with ODS (YMC-Pack A-312); mobile phase, CH_3CN-0.15 M CH_3COONH_4-CH_3COOH (45:45:10); flow rate 1.5 ml/min.

Results and Discussion

Physicochemical properties of crystalline and amorphous MAT

Fig. 2 shows the powder X-ray diffraction patterns of intact and spray-dried MAT (inlet temperature 145°C). No definite diffraction peaks were detected in the X-ray diffraction pattern of the spray-dried MAT. The amorphous state of MAT was obtained by spray drying, while the intact form showed several sharp diffraction peaks. On comparison of the IR spectra of the crystalline and amorphous solids, no distinct differences between crystalline and amorphous solids were observed, although the IR peaks of the amorphous form of MAT were slightly broadened (Fig. 3).

Fig. 4 shows the DSC curves of crystalline and amorphous MAT. The DSC curve of the crystalline MAT showed an endothermic peak at 246.0°C, ascribed to fusion of MAT. On the other hand, the amorphous MAT exhibited an exothermic peak at 144.3°C and a small jump of the heat capacity at 102.2°C. The exothermic peak was attributed to a transition from amorphous to crystalline form, since the MAT powder that was removed from the DSC furnace immediately after the appearance of the exothermic peak displayed an X-ray diffraction pattern identical to that of crystalline MAT and since the DSC curve for the heated MAT powder showed an endothermic peak of melting at 246.0°C. To investigate the nature of the shift of the DSC baseline at around 102°C, the thermal behavior of the amorphous MAT was followed closely. As shown in Fig. 5, after heating to 180°C, the jump of the heat capacity at about 102°C disappeared as a result of crystallization from the amorphous to the crystalline form. After heating to 130°C, however, no changes were discernible in the DSC curve of the second run as compared with that of the first run. This jump is a typical example of a glass transi-

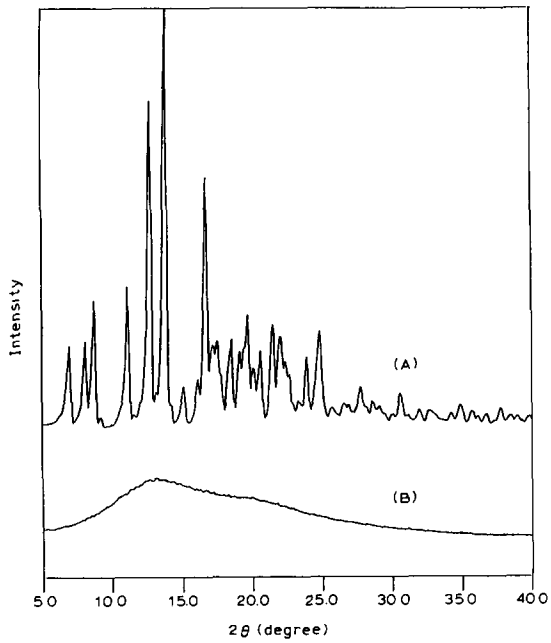

Fig. 2. Powder X-ray diffraction patterns of crystalline and amorphous MAT. (A) Crystalline; (B) amorphous, prepared by spray drying (SD-6).

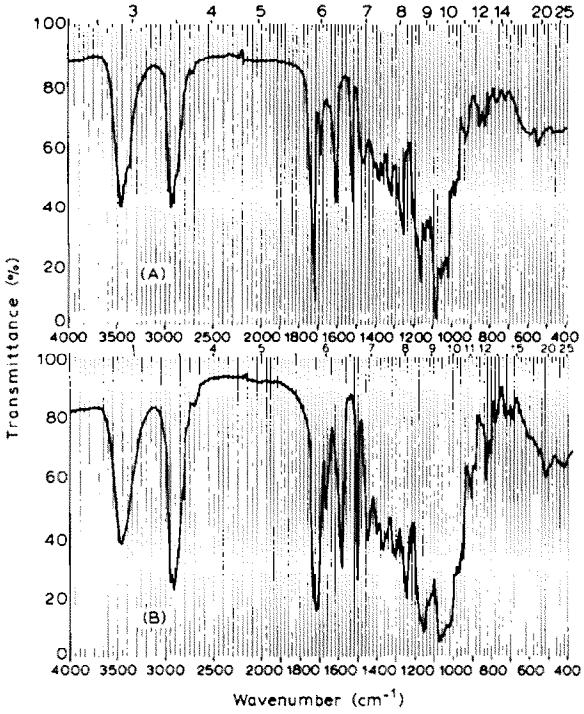

Fig. 3. IR spectra of crystalline and amorphous MAT. (A) Crystalline; (B) amorphous, prepared by spray drying (SD-6).

tion (Sakka, 1983). Fukuoka et al. (1986) reported that the glassy state of some organic compounds could be prepared by cooling of the melts. We also attempted to prepare the glass of MAT by cooling the melt of crystalline MAT and found that the specimen obtained showed thermal behavior similar to that of the powder prepared via spray drying. These results indicated that the change heat capacity of amorphous MAT was due to the glass transition. The glass transition temperature (T_g) of MAT was determined as 102°C.

Dissolution curves of the crystalline and glassy forms of MAT are shown in Fig. 6. In the case of JP 1st fluid (pH 1.2), both the crystalline solid and the glass dissolved rapidly, in process of dissolution reacting completion within 5 min. This was due to the high solubility of the basic drug in acidic solution. On the other hand, in the JP 2nd fluid (pH 6.8) and distilled water, the dissolution curves differed between the crystalline solid and the glass. In both cases, the crystalline MAT was practically insoluble and had a solubility of about 1.0 μg/ml near pH 7. The glassy MAT, however, showed behavior in line with supersaturation during the initial stages of dissolution, followed by a gradual decrease in the high concentration of MAT as a result of the recrystallization of MAT. After the dissolution experiments with JP 2nd fluid and distilled water, the precipitates were collected and dried at 60°C under reduced pressure. The powder X-ray diffraction patterns of the precipitates coincided with those of the crystalline solid.

Effect of drying temperature on the formation of amorphous MAT by spray drying

Different kinds of amorphous solids were prepared by spray drying dichloromethane solutions of MAT. Various inlet temperatures of the spray dryer were used, viz., 50, 70, 95, 102, 120, 145 and 160°C. Each spray-dried sample was designated SD-1–SD-7 in order of low inlet temperature. The residual solvent (dichloromethane) in each sample was found to be less than the limit of detection (20 ppm) of gas chromatography.

The powder X-ray diffraction patterns of each sample are depicted in Fig. 7. SD-1, which was prepared at the lowest temperature, showed small diffraction peaks of crystalline MAT, while the patterns of the other samples had a halo, indicat-

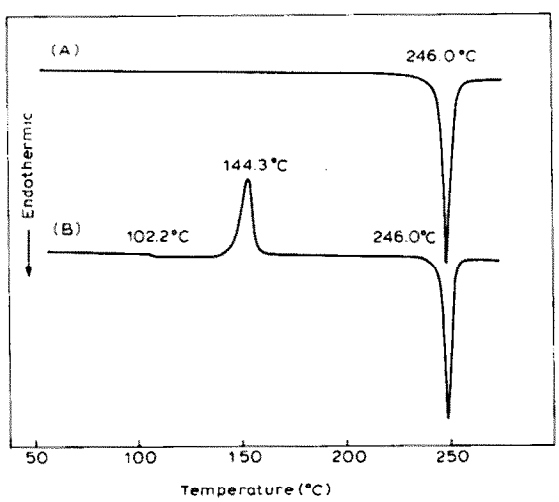

Fig. 4. DSC curves of crystalline and amorphous MAT. (A) Crystalline; (B) Amorphous, prepared by spray drying (SD-6).

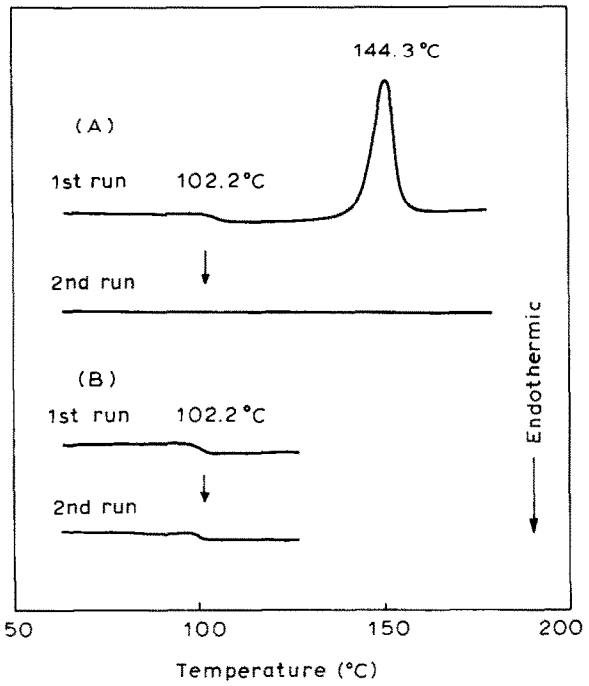

Fig. 5. Thermal behavior of amorphous MAT (SD-6). (A) DSC curves of amorphous MAT between 60 and 180°C (1st and 2nd runs); (B) DSC curves of amorphous MAT between 60° and 130°C (1st and 2nd runs).

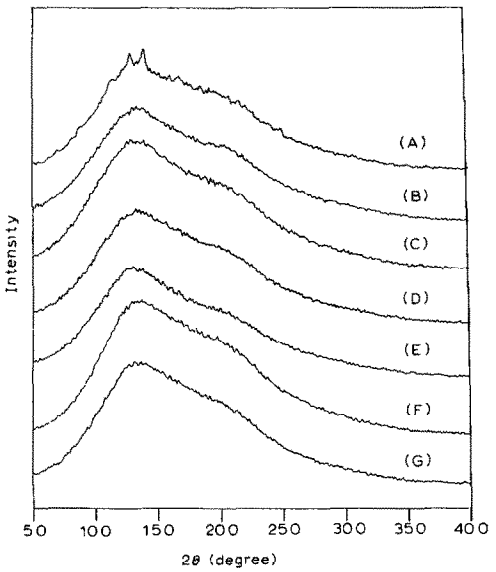

Fig. 7. Powder X-ray diffraction patterns of various spray-dried MAT. (A) SD-1 (48–55°C); (B) SD-2 (68–75°C); (C) SD-3 (95–96°C); (D) SD-4 (102–104°C); (E) SD-5 (118–120°C); (F): SD-6 (145–148°C); (G) SD-7 (160–161°C). Numbers in parentheses indicate inlet temperature of spray drying.

ing the amorphous state. In the IR spectra, no differences were discernible among the seven samples. All amorphous forms of MAT prepared by spray drying showed similar thermal behavior for the glass transition, recrystallization and melting. However, distinct differences were observed for the recrystallization temperature (T_c) and the heat of recrystallization ($|\Delta H_c|$). Fig. 8 shows the variations in the thermal parameters among the samples. The glass transition temperature (T_g) had little scatter between 101 and 103°C, while considerable variations in T_c and $|\Delta H_c|$ were observed. When the inlet temperature was

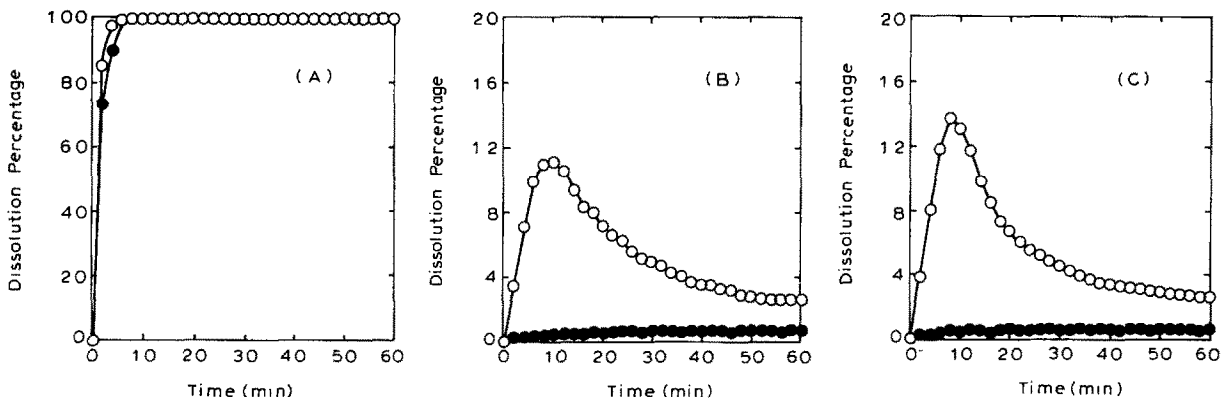

Fig. 6. Dissolution curves for crystalline and amorphous MAT (SD-6) in JP 1st fluid, JP 2nd fluid and distilled water. (A) JP 1st fluid (pH 1.2); (B) JP 2nd fluid (pH 6.8); (C) distilled water; (●) crystalline; (○) amorphous.

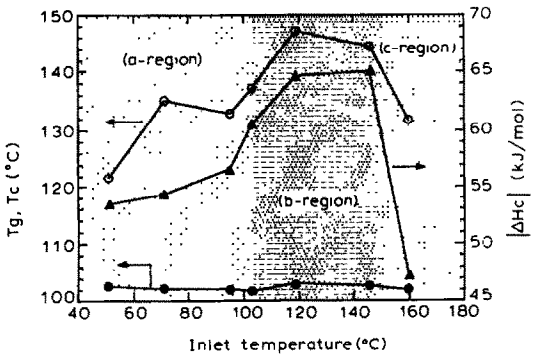

Fig. 8. Comparison of T_g, T_c and $|\Delta H_c|$ of various amorphous MAT ($n = 3$). (●——●) T_g, (○——○) T_c, (▲——▲) $|\Delta H_c|$.

lower than the T_g which was designated the a-region, both T_c and $|\Delta H_c|$ were low. At inlet temperatures intermediate between T_g and T_c (b-region), markedly higher values were observed for T_c and $|\Delta H_c|$. At the temperatures above T_c (c-region), these values were observed to decrease rapidly. The above results suggested that amorphous MAT prepared in the b-region were more stable in terms of high T_c and great $|\Delta H_c|$ than the spray-dried powders prepared in the a- and c-regions. In other words, crystalline nuclei of MAT were partially present in specimens prepared in the a- and c-regions, so that it seemed reasonable that the values of T_c and $|\Delta H_c|$ could decrease in these regions. For inlet temperatures below T_g or above T_c, it was supposed that in MAT particles there might be some kind of micro-ordered structure in a three-dimensional array of MAT molecules during the process of drying. At inlet temperatures between T_g and T_c (b-region), however, MAT should be able to form a stable glassy state which has a greater degree of disorder of the molecular arrangement in the specimen.

Microscopic observation and some other parameters

Fig. 9 shows photographs of particles of SD-2, SD-5 and SD-7. The shapes of SD-2 and SD-7 were mostly spherical, while no fixed shape was observed for SD-5. The results of microscopic observation on all samples are summarized in Table 1. The appearance of particles depended upon the inlet temperature of the spray dryer. Namely, the particles were spherically shaped at inlet temperatures below T_g (a-region). The content of spherical particles, however, decreased gradually near the T_g, and the shape of the particles changed to that of a flat thin plate (i.e., no fixed shape) above the T_g. At temperatures above T_c (c-region), the particles became spherical again. The above changes in particle shape suggested that MAT molecules existed in various cohesive states among the spray-dried powders. Table 1 also lists the apparent densities of these samples. The apparent density also depended upon the spray drying temperature. The apparent densities of the powders prepared in the b-region were lower than those of the powders prepared in a- and c-regions. Some variability in the apparent

TABLE 1

Physico-chemical properties of spray-dried MAT

Lot no.	Region	Inlet temperature (°C)	Outlet temperature (°C)	Shape of particles	Apparent density (g/cm^3)	Changes in appearance [a]	Potency (μg/mg)	Relative purity (%)
SD-1	a	48–55	–	spherical	0.275	powder	961.5	97.80
SD-2	a	68–75	–	spherical	0.262	powder	965.0	97.57
SD-3	a	95–96	45	spherical > unfixed	0.193	powder, partly shrunk	957.3	97.63
SD-4	b	102–104	60	spherical < unfixed	0.162	shrunk	959.0	97.59
SD-5	b	118–120	63	unfixed	0.133	shrunk	958.5	97.54
SD-6	b	145–148	69 ~ 73	unfixed	0.153	shrunk	966.5	97.57
SD-7	c	160–161	83 ~ 84	spherical > unfixed	0.196	powder, partly shrunk	960.3	97.57

[a] Changes in appearance of powders were observed after heating to 130°C in DSC measurements. The lids of aluminum pans were not used.

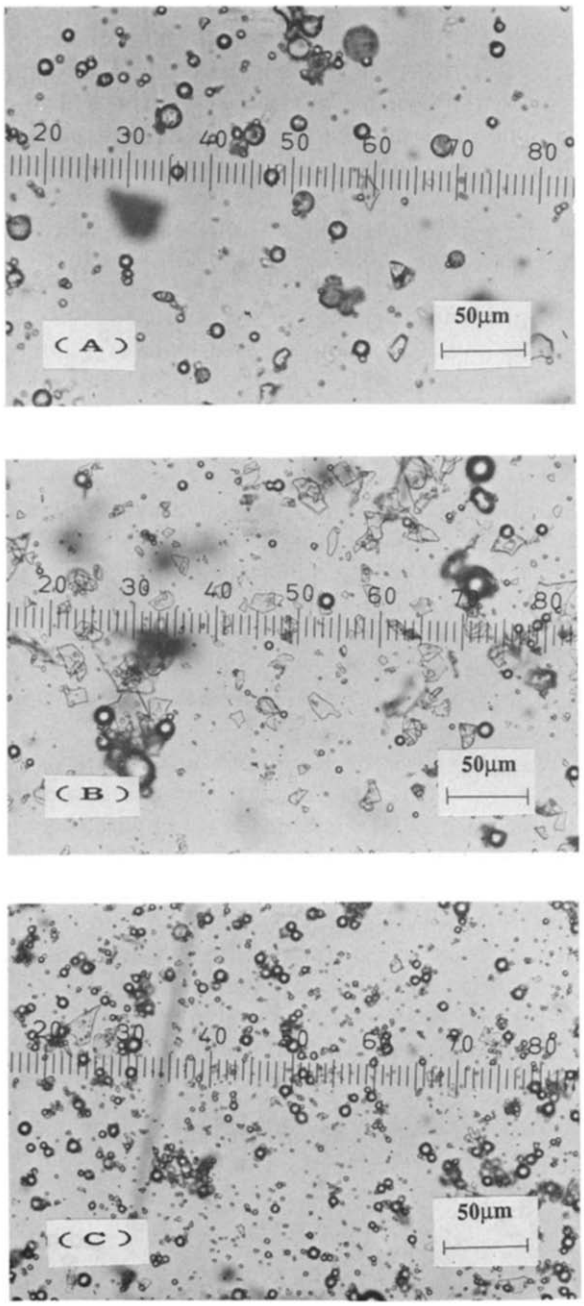

Fig. 9. Micrographs of amorphous MAT particles prepared by spray drying. (A) SD-2, (B) SD-5, (C) SD-7.

density could be attributed to the differences in particle shape.

Moreover, other morphological changes were observed during the DSC measurements of spray-dried samples. Each spray-dried powder was heated using DSC to 130°C at a heating rate of 10°C/min without a lid on the sample pan, the changes in appearance of the samples being shown in Fig. 10. SD-4–SD-6 had shrunk after heating, while the other powders (SD-1–3 and 7) remained unaffected. Generally, the glassy state was expressed as a frozen liquid, and the arrangement of the molecules in the glass showed perfect disorder as well as in the fluid, that is to say, uniform amorphous solid (Goldstein and Simha, 1976). The apparent densities of SD-4–SD-6 were rather low compared with the other powders. The observed shrinking should be ascribable to changes in the apparent volume on heating. On the other hand, the other powders (SD-1–3 and 7) were morphologically stable at temperatures higher than T_g in the DSC measurements, presumably due the partially ordered molecular orientation.

The differences in the amount of adsorbed water among the samples were not detected under conditions of 40°C and 75% RH. The results on the potency and relative purity determined via HPLC analysis are also listed in Table 1. Very little variation in potency and relative purity of samples was observed, within experimental error. Hence, the differences in physicochemical properties among spray-dried samples could not be explained in terms of the purity, residual solvent or hygroscopic properties.

Fig. 11 shows the dissolution patterns of each amorphous powder at 37 ± 0.1°C in distilled water. All samples, except for SD-1, showed behavior indicative of supersaturation during the initial stages of dissolution and the high concentration

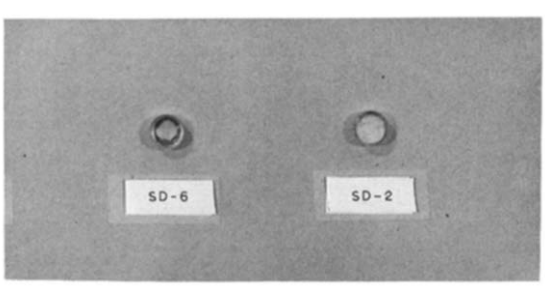

Fig. 10. Photograph of amorphous MAT (SD-2 and SD-6) after heating to 130°C.

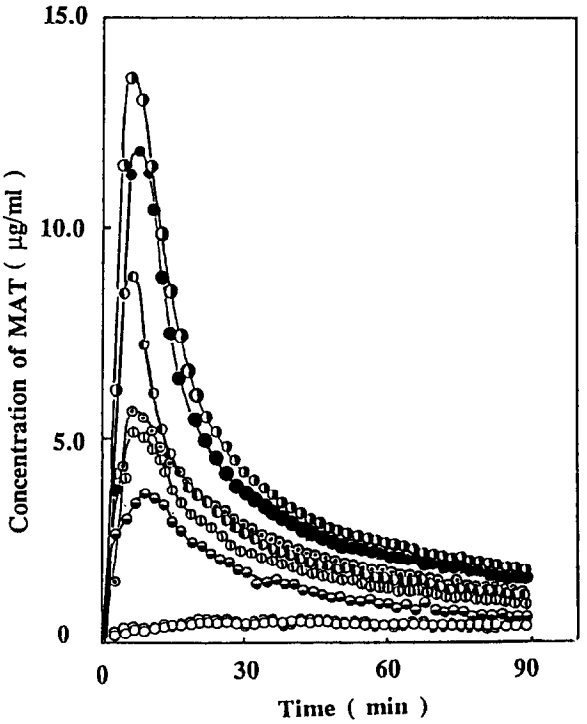

Fig. 11. Dissolution patterns of various amorphous MAT in distilled water at 37°C (paddle method, 100 rpm). (○——○) SD-1, (◒——◒) SD-2, (◑——◑) SD-3, (◐——◐) SD-4, (●——●) SD-5, (◑——◑) SD-6, (⊙——⊙) SD-7.

decreased gradually due to the recrystallization of MAT. The maximum MAT concentration observed in SD-5 and SD-6 was higher than those of other spray-dried powders. Egawa et al. (1992) reported variations in the apparent solubility levels of cefalexin using amorphous cefalexin powders and different grinding times, even though the X-ray diffractograms displayed almost identical halo patterns. Therefore, the assumption that different kinds of amorphous states of MAT can exist appears to be reasonable. Namely, they could be prepared by changing the inlet temperature of the spray dryer.

Physicochemical stability of glassy MAT

We investigated the physicochemical stability of glassy MAT (SD-1–SD-7) at 40°C and 75% RH. X-ray diffractometry and DSC were used to evaluate the crystallinity of MAT samples. The degree of crystallization of MAT was estimated based on the crystallinity index method (Walkelin et al., 1959). In this work, intact crystalline sample was used as the standard for 100% crystal, and SD-5 was selected as the standard for amorphous samples. X-ray diffraction intensities were measured at 0.04° intervals from $2\theta = 5.0$ to 40.0°, and then compared with those for standard samples at each diffraction peak.

Fig. 12 shows the X-ray diffraction patterns of SD-3, SD-5 and SD-7 for various storage times. In the case of SD-5, which was prepared at an inlet temperature between T_g and T_c (b-region), the glassy MAT was remarkably stable, and no crystalline diffraction peaks of MAT were observed even after storage for 7 weeks. SD-7, which was prepared at a temperature above T_c (c-region), was the most unstable, and crystalline diffraction peaks of MAT were evident within 1 week. In the case of SD-3, which was prepared

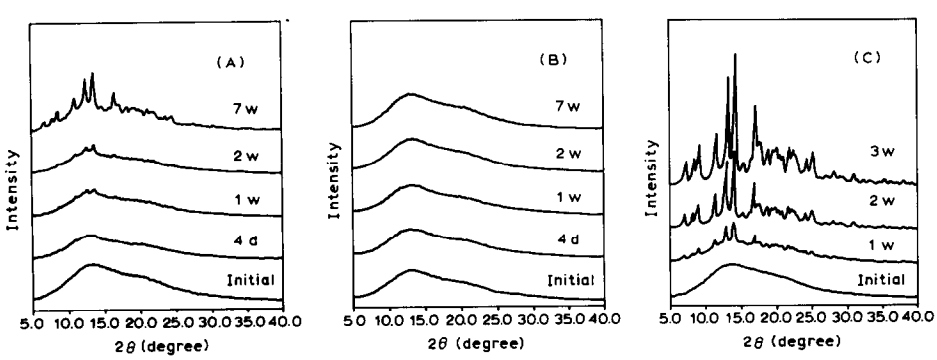

Fig. 12. Changes in powder X-ray diffraction patterns of amorphous MAT at 40°C and 75% RH. (A) SD-3, (B) SD-5, (C) SD-7.

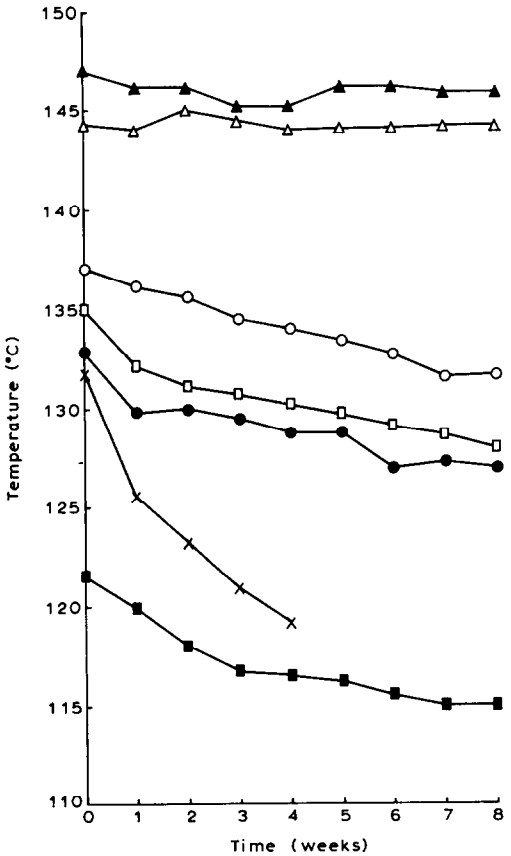

Fig. 13. Changes in T_c of amorphous MAT during storage at 40°C and 75% RH. (■ ——— ■) SD-1, (□ ——— □) SD-2, (● ——— ●) SD-3, (○ ——— ○) SD-4, (▲ ——— ▲) SD-5, (△ ——— △) SD-6, (× ——— ×) SD-7.

below T_g (a-region), the physicochemical stability of the amorphous form was not good as well as SD-7. The rate of crystallization of SD-3, however, was slower than that of SD-7. The peak position of crystalline peaks recognized for SD-3 and SD-7 corresponded with those of intact crystal. Changes in the crystallinity indices for all amorphous forms of MAT from SD-1–SD-7 during storage at 40°C and 75% RH are summarized in Table 2. As is evident from Table 2, the physicochemical stability of amorphous powders prepared at temperatures in the b-region was remarkably high while those prepared at temperatures in the c-region were the most unstable among the samples used in this work. In the case of SD-1–SD-4 prepared in the a-region, decreasing the inlet temperature caused a decrease in the physicochemical stability of the amorphous state. As shown in Figs 13 and 14, T_c and $|\Delta H_c|$ scarcely changed in the case of SD-5 and SD-6 during storage for 7 weeks, while the values for the other samples gradually decreased as a function of storage time. The changes in T_c and $|\Delta H_c|$ of amorphous MAT during storage at 40°C and 75% RH showed a close correlation with the results on crystallinity changes as indicated in Table 2. The results showed that the stability of amorphous MAT was markedly influenced by the inlet temperature of the spray dryer. The controlling of the drying temperature between T_g and T_c was essential in order to prepare stable amorphous samples.

The present results demonstrate that amorphous MAT can be prepared by spray drying a dichloromethane solution and that different kinds of glassy state can be obtained by changing the inlet temperature of the spray dryer. It was found that the greatest physicochemical stability is achieved when the amorphous powders are pre-

TABLE 2

Changes in crystallinity indices of various amorphous MAT during storage of 40°C and 75% RH

Samples	Crystallinity index (%)						
	Initial	2 days	1 week	2 weeks	4 weeks	6 weeks	8 weeks
SD-1	2	7	10	15	20	27	31
SD-2	0	4	8	10	12	17	25
SD-3	0	0	2	4	6	11	15
SD-4	0	0	0	0	0	0	7
SD-5	0	0	0	0	0	0	0
SD-6	0	0	0	0	0	0	0
SD-7	0	2	6	10	16	45	–

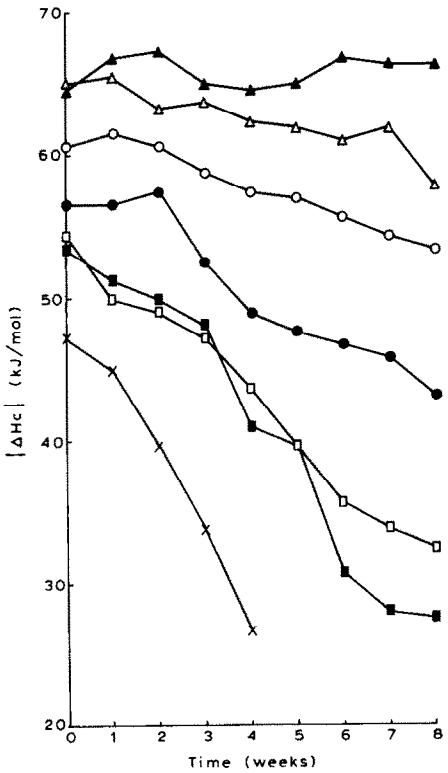

Fig. 14. Changes in enthalpy of crystallization of amorphous MAT during storage at 40°C and 75% RH. (■——■) SD-1, (□——□) SD-2, (•——•) SD-3, (○——○) SD-4, (▲——▲) SD-5, (△——△) SD-6, (×——×) SD-7.

pared at temperatures between T_g and T_c. Further investigation of the physical stability of other macrolide compounds will be reported in a subsequent paper.

Acknowledgment

The authors wish to thank Professor Eihei Fukuoka of Toho University for valuable suggestions.

References

Aoyagi, N., Ogata, H., Kaniwa, N. and Eijima, A., Bioavailability of indomethacin capsules in humans (1) Bioavailability and effects of gastric acidity, (2) Correlation with dissolution rate. *Int. J. Clin. Pharmacol. Ther. Toxicol.*, 23 (1985) 469–474; 529–534.

Baba, K., Takeichi, Y. and Nakai, Y., Molecular behavior and dissolution characteristics of uracil in ground mixtures. *Chem. Pharm. Bull.*, 38 (1990) 2542–2546.

Ballard, B.E. and Nelson, E., Physicochemical properties of drugs that control absorption rate after subcutaneous implantation. *J. Pharmacol. Exp. Ther.*, 135 (1962) 120–127.

Egawa, H., Maeda, S., Yonemochi, E., Oguchi, T., Yamamoto, K. and Nakai, Y., Solubility parameter and dissolution behavior of various cefalexin powders. *Chem. Pharm. Bull.*, 40 (1992) 819–820.

Fukuoka, E., Makita, M. and Yamamura, S., Glassy state of pharmaceuticals. III. Thermal properties and stability of glassy pharmaceuticals and their binary glass systems; IV: Studies on glassy pharmaceuticals by thermomechanical analysis. *Chem. Pharm. Bull.*, 37 (1989) 1047–1050; 2782–2785.

Fukuoka, E., Makita, M. and Yamamura, S., Some physicochemical properties of glassy indomethacin. *Chem. Pharm. Bull.*, 34 (1986) 4314–4321.

Goldstein, M. and Simha, R., The glass transition and the nature of the glassy states. *Ann. NY Acad. Sci.*, 279 (1976).

Haleblian, J. and McCrone, W., Pharmaceutical applications of polymorphism. *J. Pharm. Sci.*, 58 (1969) 911–929.

Kawashima, Y., Niwa, T., Takeuchi, H., Hino, T., Itoh, Y. and Furuyama, S., Characterization of polymorphs of tranilast anhydrate and tranilast monohydrate when crystallized by two solvent charge spherical crystallization techniques. *J. Pharm. Sci.*, 80 (1991) 472–478.

Lindenbaum, J., Butler, Jr. V.P., Murphy, J.E. and Cresswell, R.M., Correlation of digoxin-tablet dissolution-rate with biological availability. *Lancet* 1 (1973) 1215–1217.

Morishita, M., Ohno, M., Ohta, K., Sumita, Y., Matsumura, T. and Suzuki, T., Formulation design of rokitamycin tablet and its evaluation. *Yakuzaigaku*, 48 (1988) 154–163.

Mullins, J.D. and Macek, T.J., Some pharmaceutical properties of novobiocin. *J. Am. Pharm. Assoc.*, 49 (1960) 245–248.

Nakai, Y., Molecular behavior of medicinals in ground mixtures with microcrystalline cellulose and cyclodextrins. *Drug Dev. Ind. Pharm.*, 12 (1986) 1017–1039.

Sakka, S., *Galasu hishoushitsu no kagaku*, Uchida Rokakuho, 1983, pp. 251–271.

Sato, T., Okada, A., Sekiguchi, K. and Tsuda, Y., Difference in physico-pharmaceutical properties between crystalline and noncrystalline 9,3″-diacetylmidecamycin. *Chem. Pharm. Bull.*, 29 (1981) 2675–2682.

Tsuchiya, M., Hamada, M., Takeuchi, T., Umezawa, H., Yamamoto, K., Tanaka, H., Kiyoshima, K., Mori, S. and Okamoto, R., Studies of tylosin derivatives effective against macrolide-resistant strains: Synthesis and structure-activity relationships. *J. Antibiot.*, 35 (1982) 661–672.

Wakelin, J.H., Virgin, H.S. and Crystal, E., Development and comparison of two X-ray methods for determining the crystallinity of cotton cellulose. *J. Appl. Phys.*, 30 (1959) 1654–1662.

Yamamoto, K., Nakano, M., Arita, T., Takayama, Y. and Nakai, Y., Dissolution behavior and bioavailability of phenytoin from a ground mixture with microcrystalline cellulose. *J. Pharm. Sci.*, 65 (1976) 1484–1488.